

*Regular article*

# Efficient electronic structure calculations for systems of one-dimensional periodicity with the restricted Hartree–Fock–linear combination of atomic orbitals method implemented in Fourier space

I. Flamant<sup>1</sup>, J. G. Fripiat<sup>2</sup>, J. Delhalle<sup>1</sup>, Frank E. Harris<sup>3,4</sup>

<sup>1</sup>Laboratoire Interdisciplinaire de Spectroscopie Electronique, Facultés Universitaires Notre-Dame de la Paix, Rue de Bruxelles 61, 5000 Namur, Belgium

<sup>2</sup>Laboratoire de Chimie Théorique Appliquée, Facultés Universitaires Notre-Dame de la Paix, Rue de Bruxelles 61, 5000 Namur, Belgium

<sup>3</sup>Department of Physics, University of Utah, Salt Lake City, UT 84112, USA

<sup>4</sup>Quantum Theory Project, University of Florida, P.O. Box 118435, Gainesville, FL 32611, USA

Received: 20 August 1999 / Accepted: 17 January 2000 / Published online: 5 June 2000

© Springer-Verlag 2000

**Abstract.** Formulas are presented for restricted Hartree–Fock (RHF) calculations on systems with periodicity in one dimension using a basis set of contracted spherical Gaussians. Applying Fourier-space and Ewald-type methods, all lattice sums appearing in the formulation have been brought to forms exhibiting accelerated convergence. Calculations have been carried out for infinite chains of Li<sub>2</sub> molecules and a poly(oxy-methylene) chain. The methods used here yield results that are far more precise than corresponding direct-space calculations and for the first time show the vanishing of the RHF density of states at the Fermi level for situations of partial band occupancy. Our initial computational implementation was about 5 times slower than the fastest direct-space RHF code, but improvements in special-function evaluations and numerical integrations over the Brillouin zone are shown to remove this disparity in computing speed.

**Key words:** Restricted Hartree–Fock – Fourier space – Gaussian-type functions – Polymers – Band structure

## 1 Introduction

Quantum mechanical calculations for systems with periodicity in one dimension provide important support for the interpretation and prediction of the electronic and molecular structures of large regular oligomers and polymers [1]. In that context, Hartree–Fock-based methods are central since they often constitute a reference for the more approximate approaches and a consistent starting point for those going beyond the single determinant level.

Common to methods for periodic systems is the occurrence of lattice sums which can lead to ambiguous results when not evaluated to suitable convergence. Numerous contributions have been published on truncations and/or approximate schemes to circumvent the convergence problems [2–6]. These investigations have essentially been made for the direct-space linear combination of atomic orbitals (LCAO) realisation of the restricted Hartree–Fock (RHF) method (RHF-LCAO) when Gaussian-type basis functions are used. Though substantial improvements have been noted with these schemes they remain unsatisfactory because of the absence of control of the accuracy and lack of balance among the various contributions.

It is only recently that the Fourier-space formulation of the RHF-LCAO method [7] for systems with periodicity in one dimension [8–10] has been considered to deal with the lattice summations of both the classical electrostatic and exchange terms. A method based on a combination of the Poisson formula and the Ewald technique has been developed to compute these lattice summations consistently to within a specified numerical accuracy [11, 12]. The method has been implemented in a prototype computer program (FTCHAIN) using s-type Gaussian basis functions. Comparative studies [12–16] with the PLH direct-space code [17] have proved the efficiency and stability of the Fourier-space method in situations where both approaches normally provide comparable results, i.e. large-gap systems and localised atomic bases. Even in such favourable situations, the tests have revealed that the direct-space code has unexpected difficulties in providing converged classical electrostatic and exchange lattice-sum contributions. For instance, in the case of the poly(oxy-methylene) chain,  $-(\text{CH}_2-\text{O})_x-$ , discrepancies between the results obtained from PLH (with lattice summations carried out as accurately as that code presently permits) and

FTCHAIN occur in the third significant digit [12, 16]. These differences are of Coulombic as well as exchange nature and can be reduced below the sixth significant digit only by using increasingly localised atomic functions. Furthermore, a significant achievement possible with the Fourier-space approach, not attained so far with direct-space codes, is the ability to yield the vanishing of the RHF density of states at the Fermi level in situations of partial band occupancy [12–14].

The present Fourier-space implementation leads, however, to computing times 5 times longer than with the PLH code (probably the most efficient to date for one-dimensional systems) [17]. Another point still unsolved is the control of accuracy in the integration over the Brillouin zone (BZ).

One purpose of this contribution is to propose directions to make the Fourier-space algorithm competitive with corresponding direct-space codes such as PLH and CRYSTAL95 [18]. The article begins with a brief overview of the basic Fourier-space RHF-LCAO equations (Sect. 2), following which working expressions are provided for the case of s-type Gaussian functions (Sect. 3). An analysis in Sect. 4 shows that computation of electron–electron interaction can be improved in at least two ways. Practical methods are proposed for accomplishing this.

## 2 Fourier-space RHF-LCAO expressions for systems of one-dimensional periodicity

In the RHF approximation, the electronic wave function is a Slater determinant built from one-electron orbitals of Bloch type. The RHF–Bloch orbitals,  $\varphi_n(k, \mathbf{r})$ , are doubly occupied up to the Fermi energy,  $E_F$ , and are orthonormalised as shown in the following equation

$$\langle \varphi_{n'}(k', \mathbf{r}) | \varphi_n(k, \mathbf{r}) \rangle = \delta_{k'k} \delta_{n'n} , \quad (1)$$

where  $k$  and  $n$  are the wavenumber and the band index, respectively. In the notation used here,  $k$  is expressed in units of  $2\pi/s_0$ ,  $s_0$  being the cell length, and is defined in the BZ, whose length is  $2\pi/s_0$ , i.e.,  $k \in [-1/2, 1/2]$ . The Bloch orbitals

$$\varphi_n(k, \mathbf{r}) = \sum_p c_{pn}(k) b_p(k, \mathbf{r}) \quad (2)$$

are expressed in terms of Bloch sums  $b_p(k, \mathbf{r})$

$$\begin{aligned} b_p(k, \mathbf{r}) &= (2N + 1)^{-1/2} \sum_m \exp(i2\pi mk) \chi_p[\mathbf{r} - (\mathbf{p} + m\mathbf{e}_z)s_0] \\ &= (2N + 1)^{-1/2} \sum_m \exp(i2\pi mk) \chi_p^m(\mathbf{r}) , \end{aligned} \quad (3)$$

where  $p$  and the vector  $\mathbf{p}$  (in units of cell length  $s_0$ ), respectively, represent the label and the position of atomic orbital  $\chi_p$  in the reference unit cell. The quantity  $(2N + 1)^{-1/2}$  is the normalisation factor for a polymer containing  $2N + 1$  ( $N \rightarrow \infty$ ) unit cells. In the following, the indices  $p, q, r$  and  $s$  denote atomic orbitals and the number of electrons per unit cell is  $n_e$ . The direction of periodicity is defined by the unit vector  $\mathbf{e}_z$  and the lattice sites are identified by integers  $m, m'$  and  $m''$  (with values  $0, \pm 1, \pm 2, \dots, \pm N$ ).

The normalization condition, in terms of Bloch sums and for  $n = n'$  and  $k = k'$ , is

$$\begin{aligned} \sum_{p,q} c_{pn}^*(k) \langle b_p(k, \mathbf{r}) | b_q(k, \mathbf{r}) \rangle c_{qn}(k) &= \sum_{p,q} c_{pn}^*(k) S_{pq}(k) c_{qn}(k) \\ &= 1 , \end{aligned} \quad (4)$$

where  $S_{pq}(k)$  are the overlap matrix elements

$$S_{pq}(k) = \langle b_p(k, \mathbf{r}) | b_q(k, \mathbf{r}) \rangle . \quad (5)$$

The density matrix elements,  $P_{pq}(k)$ , are given by

$$P_{pq}(k) = \sum_n c_{pn}^*(k) c_{qn}(k) \theta_n(k) , \quad (6)$$

with the occupation function,  $\theta_n(k)$ , defined as

$$\theta_n(k) = \begin{cases} 2 & \text{if } E_n(k) \leq E_F \\ 0 & \text{if } E_n(k) > E_F \end{cases} ,$$

where  $E_n(k)$  is the energy of band  $n$ .

The expansion coefficients,  $c_{pn}(k)$ , and the one-electron energy eigenvalues,  $E_n(k)$ , are solutions of the following system of equations

$$\sum_q F_{pq}(k) c_{qn}(k) = E_n(k) \sum_q S_{pq}(k) c_{qn}(k) , \quad (7)$$

in which  $F_{pq}(k)$  are the Fock matrix elements given by

$$F_{pq}(k) = T_{pq}(k) + C_{pq}(k) + X_{pq}(k) , \quad (8)$$

where  $C_{pq}(k) = V_{pq}(k) + J_{pq}(k)$ .  $T_{pq}(k)$  is the kinetic energy term,

$$T_{pq}(k) = \langle b_p(k, \mathbf{r}) | -\frac{1}{2} \nabla_{\mathbf{r}}^2 | b_q(k, \mathbf{r}) \rangle , \quad (9)$$

$V_{pq}(k)$  is the electron–nuclear attraction term,

$$\begin{aligned} V_{pq}(k) &= - \left\langle b_p(k, \mathbf{r}) \left| \sum_A Z_A \sum_{m'} |\mathbf{r} - (\mathbf{A} + m'\mathbf{e}_z)s_0|^{-1} \right. \right. \\ &\quad \left. \left. \times b_q(k, \mathbf{r}) \right\rangle , \end{aligned} \quad (10)$$

$J_{pq}(k)$  is the electron–electron repulsion term,

$$J_{pq}(k) = (2N + 1) \int_{\text{BZ}} dk' \sum_{r,s} P_{rs}(k') J_{pqrs}(k, k') , \quad (11)$$

where

$$\begin{aligned} J_{pqrs}(k, k') &= \iint d\mathbf{r}_1 d\mathbf{r}_2 b_p^*(k, \mathbf{r}_1) b_q(k, \mathbf{r}_1) |\mathbf{r}_1 - \mathbf{r}_2|^{-1} \\ &\quad \times b_r^*(k', \mathbf{r}_2) b_s(k', \mathbf{r}_2) , \end{aligned} \quad (12)$$

and  $X_{pq}(k)$  is the exchange term,

$$X_{pq}(k) = -\frac{1}{2} (2N + 1) \int_{\text{BZ}} dk' \sum_{r,s} P_{rs}(k') X_{psrq}(k, k') , \quad (13)$$

where

$$\begin{aligned} X_{psrq}(k, k') &= \iint d\mathbf{r}_1 d\mathbf{r}_2 b_p^*(k, \mathbf{r}_1) b_s(k', \mathbf{r}_1) |\mathbf{r}_1 - \mathbf{r}_2|^{-1} \\ &\quad \times b_r^*(k', \mathbf{r}_2) b_q(k, \mathbf{r}_2) . \end{aligned} \quad (14)$$

$Z_A$  and the vector  $\mathbf{A}$  (in units of cell length  $s_0$ ) are the charge and the position of nucleus  $A$ , respectively.

In the Fourier space, the expression for the Coulomb term,  $C_{pq}(k)$ , is

$$C_{pq}(k) = (\pi s_0)^{-1} \sum_{m'} \int \frac{d\mathbf{q}_0}{q_0^2 + m'^2} S_{pq}(k, \mathbf{q}_{m'}) \times \left[ \int_{\text{BZ}} d\mathbf{k}' \left( \sum_{r,s} P_{rs}(k') S_{rs}(k', -\mathbf{q}_{m'}) \right) - \sum_A Z_A \exp(-i2\pi \mathbf{q}_{m'} \cdot \mathbf{A}) \right], \quad (15)$$

where  $q_0^2 = q_x^2 + q_y^2$ ,  $\mathbf{q}_{m'} = (q_x, q_y, m')$  and  $d\mathbf{q}_0 = dq_x dq_y$ ,  $\mathbf{q}$  being the Fourier transform variable. The exchange term in Fourier space is written as

$$X_{pq}(k) = -\frac{1}{2} (\pi s_0)^{-1} \int_{\text{BZ}} d\mathbf{k}' \sum_{r,s} P_{rs}(k') \times \sum_m \int \frac{d\mathbf{q}_0}{q_0^2 + (m+k-k')^2} S_{ps}(k', \mathbf{q}_{m+k-k'}) \times S_{rq}(k, -\mathbf{q}_{m+k-k'}) , \quad (16)$$

in which  $\mathbf{q}_{m+k-k'} = (q_x, q_y, m+k-k')$ . In Eqs. (15) and (16),  $S_{pq}(k, \mathbf{q})$  are the generalized overlap matrix elements,

$$S_{pq}(k, \mathbf{q}) = \sum_m \exp(i2\pi mk) \times \left\langle \chi_p^0 \left| \exp\left(i \frac{2\pi}{s_0} \mathbf{q} \cdot \mathbf{r}\right) \right| \chi_q^m \right\rangle . \quad (17)$$

### 3 Matrix elements for s-type Gaussian atomic basis sets

The explicit forms for the quantities needed in actual calculations using s-type Gaussian basis functions are provided here without detailed derivation: this can be found in Ref. [12]. The obvious cases such as overlap and kinetic energy matrix elements are not reproduced here. In the case of a contracted basis set of s-type Gaussian atomic orbitals, the Coulomb term is written as

$$C_{pq}(k) = \sum_{a=1}^{\omega_p} \sum_{b=1}^{\omega_q} D_{ap} D_{bq} C_{ab}(k) , \quad (18)$$

with

$$C_{ab}(k) = \int_{\text{BZ}} d\mathbf{k}' \sum_{r,s} P_{rs}(k') \sum_{c=1}^{\omega_r} \sum_{d=1}^{\omega_s} D_{cr} D_{ds} C_{abcd}(k, k') . \quad (19)$$

The indices  $a, b, c$  and  $d$  refer to the Gaussian functions,  $\omega_p$  is the number of primitives in the expansion representing the atomic orbital  $p$  and  $D_{ap}$  is the contraction coefficient. In the expressions which follow,  $\alpha_a$  is the exponent of a Gaussian function and  $\mathbf{a}$  the location of its centre in units of  $s_0$ , with decomposition  $\mathbf{a} = \mathbf{a}_0 + \alpha_z \mathbf{e}_z$  to the  $xy$ -plane and  $z$  projections. The Coulomb integrals,  $C_{abcd}(k, k')$ , are expressed as

$$C_{abcd}(k, k') = (\pi s_0)^{-1} S_{ab}^{(x,y)} S_{cd}^{(x,y)} I_C(k, k') , \quad (20)$$

with

$$S_{ab}^{(x,y)} = \left( \frac{\pi}{\alpha_a + \alpha_b} \right) \exp\left( -\frac{\alpha_a \alpha_b}{\alpha_a + \alpha_b} (\mathbf{b}_0 - \mathbf{a}_0)^2 s_0^2 \right) . \quad (21)$$

Due to the use of Poisson summation and Ewald techniques for efficient calculation of lattice sums, the Coulomb contribution,  $I_C(k, k') = I_C^V(k, k') + I_C^J(k, k')$ , is split in two parts:  $I_C^V(k, k')|_0^{\tau_2}$  and  $I_C^J(k, k')|_0^{\tau_1}$ . The explicit forms of the individual terms are given below.

In the interval  $[0, \tau_1]$ , the electron–electron repulsion part of the Coulomb term is written as

$$I_C^J(k, k')|_0^{\tau_1} = 2\pi^{3/2} \sum_m \sum_{m''} \exp(i2\pi mk) \exp(i2\pi m'' k') S_{ab,m}^{(z)} S_{cd,m''}^{(z)} \times \sum_{m'} \left[ \frac{1}{\sqrt{\gamma}} F_0\left( \frac{\pi^2}{\gamma} (\mathbf{P} - \mathbf{Q} - m' \mathbf{e}_z)^2 \right) - \frac{1}{\sqrt{\gamma + \tau_1}} F_0\left( \frac{\pi^2}{\gamma + \tau_1} (\mathbf{P} - \mathbf{Q} - m' \mathbf{e}_z)^2 \right) \right] \quad (22)$$

and the electron–nuclear attraction part is

$$I_C^V(k, k')|_0^{\tau_2} = -2\pi^{3/2} \sum_m \sum_{m''} \exp(i2\pi mk) \exp(i2\pi m'' k') S_{ab,m}^{(z)} S_{cd,m''}^{(z)} \times \sum_{m'} n_e^{-1} \sum_A Z_A \left[ \frac{1}{\sqrt{\delta}} F_0\left( \frac{\pi^2}{\delta} (\mathbf{P} - \mathbf{A} - m' \mathbf{e}_z)^2 \right) - \frac{1}{\sqrt{\delta + \tau_2}} F_0\left( \frac{\pi^2}{\delta + \tau_2} (\mathbf{P} - \mathbf{A} - m' \mathbf{e}_z)^2 \right) \right] , \quad (23)$$

where

$$S_{ab,m}^{(z)} = \left( \frac{\pi}{\alpha_a + \alpha_b} \right)^{1/2} \exp\left( -\frac{\alpha_a \alpha_b}{\alpha_a + \alpha_b} (m + b_z - a_z)^2 s_0^2 \right) \quad (24)$$

and where

$$\mathbf{P} = \frac{\alpha_a \mathbf{a} + \alpha_b (\mathbf{b} + m \mathbf{e}_z)}{\alpha_a + \alpha_b} \quad (25)$$

$$\mathbf{Q} = \frac{\alpha_c \mathbf{c} + \alpha_d (\mathbf{d} + m'' \mathbf{e}_z)}{\alpha_c + \alpha_d} . \quad (26)$$

The  $xy$  and  $z$  projections of  $\mathbf{P}$  are  $\mathbf{P}_0$  and  $P_z$ .  $F_0(x)$  is a function related to the error function,  $\text{erf}(x)$ ,

$$F_0(\alpha) = \frac{1}{2} \sqrt{\frac{\pi}{\alpha}} \text{erf}(\sqrt{\alpha}) \quad (27)$$

and,  $\gamma$  and  $\delta$  depend on the Gaussian exponents,

$$\gamma = \frac{\pi^2}{s_0^2} \left( \frac{1}{\alpha_a + \alpha_b} + \frac{1}{\alpha_c + \alpha_d} \right) \quad (28)$$

$$\delta = \frac{\pi^2}{s_0^2} \left( \frac{1}{\alpha_a + \alpha_b} \right) .$$

In the interval  $[\tau_1, \infty]$  or  $[\tau_2, \infty]$ , the contributions where  $m' \neq 0$  and  $m'' = 0$  have to be separated. Indeed, these

expressions include a function which diverges at  $m' = 0$ . For  $m' \neq 0$ , the electron–electron repulsion and electron–nuclear attraction terms can be treated separately, leaving a remainder,  $I_C^0(k, k')$ , constituting the combined  $m' = 0$  terms. Thus,

$$I_C(k, k')|_{\tau}^{\infty} = I_C^J(k, k')|_{\tau_1}^{\infty} + I_C^V(k, k')|_{\tau_2}^{\infty} + I_C^0(k, k') \quad (29)$$

in which

$$\begin{aligned} I_C^J(k, k')|_{\tau_1}^{\infty} &= \pi \sum_{m' \neq 0} S_{ab}^{(z)}(k, m') S_{cd}^{(z)}(k', -m') \exp[i2\pi m'(P_z - Q_z)] \\ &\times K_0\left((\gamma + \tau_1)m'^2, \frac{\pi^2(\mathbf{P}_0 - \mathbf{Q}_0)^2}{\gamma + \tau_1}\right), \end{aligned} \quad (30)$$

and

$$\begin{aligned} I_C^V(k, k')|_{\tau_2}^{\infty} &= -\pi n_e^{-1} S_{cd}^{(z)}(k', 0) \sum_{m' \neq 0} S_{ab}^{(z)}(k, m') \\ &\times \sum_A Z_A \exp[i2\pi m'(P_z - A_z)] \\ &\times K_0\left((\delta + \tau_2)m'^2, \frac{\pi^2(\mathbf{P}_0 - \mathbf{A}_0)^2}{\delta + \tau_2}\right). \end{aligned} \quad (31)$$

In these expressions,  $K_0(x, y)$  denotes the incomplete Bessel function [19]

$$K_0(x, y) = \int_1^{\infty} \exp\left(-xt - \frac{y}{t}\right) \frac{dt}{t}. \quad (32)$$

The  $z$  components of the generalized overlap matrix elements,  $S_{ab}^{(z)}(k, m')$ , are calculated using the expression

$$S_{ab}^{(z)}(k, m') = \sum_m \exp\left[i2\pi m\left(k + \frac{\alpha_b}{\alpha_a + \alpha_b} m'\right)\right] S_{ab,m}^{(z)} \quad (33)$$

or

$$\begin{aligned} S_{ab}^{(z)}(k, m') &= \frac{\pi}{s_0 \sqrt{\alpha_a \alpha_b}} \sum_m \exp\left[i2\pi\left(m + k + \frac{\alpha_b}{\alpha_a + \alpha_b}\right)(a_z - b_z)\right] \\ &\times \exp\left[-\frac{\pi^2}{s_0^2} \frac{\alpha_a + \alpha_b}{\alpha_a \alpha_b} \left(k + m + \frac{\alpha_b m'}{\alpha_a + \alpha_b}\right)^2\right] \end{aligned} \quad (34)$$

whichever provides the rapider convergence for the current Gaussian-type orbital parameters.

The  $J$  and  $V$  terms constituting the  $m' = 0$  contribution  $I_C^0(k, k')$  individually exhibit singular behaviour because  $K_0(x, y)$  diverges for  $x \rightarrow 0$ . We see from the following expression

$$K_0(x, y) = 2K_0(2\sqrt{xy}) - E_1(y) - \sum_{v=1}^{\infty} \frac{(-x)^v}{v!} E_{v+1}(y), \quad (35)$$

where the  $E_n(y)$  are exponential integral functions [20], that the divergence is that of  $K_0(z)$ , a modified Bessel

function of the second kind [20], which for small arguments,  $z$ , behaves as

$$K_0(z) \sim -\ln\left(\frac{1}{2}z\right) - \gamma_e, \quad (36)$$

where  $\gamma_e$  is the Euler constant.

The singularity in the terms of  $I_C^0(k, k')$ , however, is removed by their combination, which leads to the finite contribution

$$\begin{aligned} I_C^0(k, k') &= \pi S_{ab}^{(z)}(k, 0) S_{cd}^{(z)}(k', 0) \\ &\times \left\{ -\ln(\mathbf{P}_0 - \mathbf{Q}_0)^2 - E_1\left(\frac{\pi^2(\mathbf{P}_0 - \mathbf{Q}_0)^2}{\gamma + \tau_1}\right) + n_e^{-1} \right. \\ &\times \left. \sum_A Z_A \left[ \ln(\mathbf{P}_0 - \mathbf{A}_0)^2 + E_1\left(\frac{\pi^2(\mathbf{P}_0 - \mathbf{A}_0)^2}{\delta + \tau_2}\right) \right] \right\}. \end{aligned} \quad (37)$$

When  $\mathbf{P}_0 - \mathbf{Q}_0$  is also zero,  $\ln(\mathbf{P}_0 - \mathbf{Q}_0)^2 + E_1\left(\frac{\pi^2(\mathbf{P}_0 - \mathbf{Q}_0)^2}{\gamma + \tau_1}\right)$  must be replaced by  $-\gamma_e + \ln((\gamma + \tau_1)/\pi^2)$ ; a similar remark applies to  $\mathbf{P}_0 - \mathbf{A}_0$ .

For s-type Gaussian atomic orbitals, the exchange term,  $X_{pq}(k)$ , is written as

$$\begin{aligned} X_{pq}(k) &= -\frac{1}{2} \sum_{a=1}^{\omega_p} \sum_{d=1}^{\omega_q} D_{ap} D_{dq} \int_{\text{BZ}} dk' \sum_{r,s} P_{rs}(k') \\ &\times \sum_{c=1}^{\omega_r} \sum_{b=1}^{\omega_s} D_{cr} D_{bs} X_{abcd}(k, k'). \end{aligned} \quad (38)$$

The exchange integrals are expressed as

$$\begin{aligned} X_{abcd}(k, k') &= (\pi s_0)^{-1} S_{ab,0}^{(x,y)} S_{cd,0}^{(x,y)} \\ &\times (I_X(k, k')|_0^{\tau} + I_X(k, k')|_{\tau}^{\infty}), \end{aligned} \quad (39)$$

with

$$\begin{aligned} I_X(k, k')|_0^{\tau} &= 2\pi^{3/2} \sum_{m'} \sum_{m''} \exp(i2\pi m' k') \\ &\times \exp(i2\pi m'' k) S_{ab,m'}^{(z)} S_{cd,m''}^{(z)} \\ &\times \sum_m \exp(i2\pi m(k - k')) \\ &\times \left[ \frac{1}{\sqrt{\gamma}} F_0\left(\frac{\pi^2}{\gamma} (\mathbf{P} - \mathbf{Q} - m\mathbf{e}_z)^2\right) \right. \\ &\left. - \frac{1}{\sqrt{\gamma + \tau}} F_0\left(\frac{\pi^2}{\gamma + \tau} (\mathbf{P} - \mathbf{Q} - m\mathbf{e}_z)^2\right) \right] \end{aligned} \quad (40)$$

and

$$\begin{aligned} I_X(k, k')|_{\tau}^{\infty} &= \pi \sum_m S_{ab}^{(z)}(k', m + k - k') S_{cd}^{(z)}(k, -(m + k - k')) \\ &\times \exp(i2\pi(m + k - k')(P_z - Q_z)) \\ &\times K_0\left((\gamma + \tau)(m + k - k')^2, \frac{\pi^2(\mathbf{P}_0 - \mathbf{Q}_0)^2}{\gamma + \tau}\right). \end{aligned} \quad (41)$$

As explained in Ref. [11] (see Eq. 29), the selection of  $\tau$  values is made in such a way as to secure a balanced and still very fast convergence for the lattice sums arising in each interval i.e.  $[0, \tau]$  and  $[\tau, \infty]$ .

#### 4 Computational aspects

The calculations with the FTCHAIN program proceed as depicted schematically in Fig. 1. The steps that consume the most computer time correspond to the evaluation of the numerous two-electron integrals, of which the exchange integrals represent approximately 90% of the total effort. Common to all ab initio procedures,  $\omega$ , the total number of basis functions, is responsible for the quality of the RHF results via the LCAO representation of the one-electron states,  $\varphi_n(k, \mathbf{r})$ . It leads to a growth in the number of two-electron integrals roughly proportional to  $\omega^4$ . In the Fourier space, it is crucial to keep  $n_k$  (the number of  $k$  points in half the BZ) under control, since it contributes an additional  $n_k^2$  factor to the growth of the number of two-electron integrals. The equivalent of the  $n_k^2$  factor in direct space is  $(2N + 1)^3$ , where  $(2N + 1)$  is the number of interacting cells.

Keeping the same accuracy thresholds as in our previous work [12–16], i.e. enforcing an accuracy of ten decimal digits in the various integrals (overlap, kinetic, Coulomb and exchange), our efforts to improve the computational efficiency will be on two points: the evaluation of the two-electron integrals and numerical integration over  $k$  and  $k'$ .

To check the resulting improvements we consider two test cases: the infinite chain of lithium molecules,

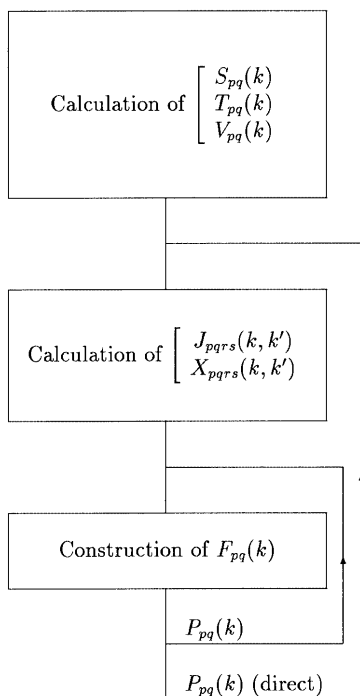


**Fig. 1.** Flow chart of the Fourier-space restricted Hartree-Fock implementation (the FTCHAIN code)

—(Li<sub>2</sub>)<sub>x</sub>—, and the poly(oxyethylene) chain, —(CH<sub>2</sub>—O)<sub>x</sub>—, a more realistic case. In the case of the lithium chains, the distance between the lithium atoms in the unit cell is arbitrarily fixed at 5.0 au. Three values of the unit cell length are considered here,  $a_0 = 10.0, 10.2$  and 12.0 au, which correspond to an even distribution of the lithium atoms along the chain and a symmetry constrained to the metallic situation, a very slightly alternating case and a more alternating situation, respectively. Calculations were carried out using two s atomic functions on each atom and the STO-3G basis set. The Slater exponents used for the STO-3G expansions of the Li<sub>1s</sub> and Li<sub>2s</sub> orbitals are 2.69 and 0.80, respectively. For the poly(oxyethylene), a distributed basis set of s-type Gaussian functions (DSGF basis set) to simulate p-type functions was used. The exponents and positions of the basis functions are listed in Table 1. The geometry of the poly(oxyethylene) chain is the same as in Ref. [16], where the unit cell length is 4.414704 au.

Three indicators will be considered: energy band values at selected  $k$  points,  $E_n(k)$ , total energy,  $E_T$ , and the computing time ratio,  $r_{CPU}$ .

#### 4.1 Computation of the two-electron integrals

Special attention was paid to the implementation of the procedure for the lattice summations occurring in the working expressions for the two-electron integrals and the choice of approaches for the efficient computation of well-known special functions, such as the  $F_0(x)$  function. On the other hand, at the time the bulk of the present work was carried out, we did not have in hand an efficient algorithm for the computation of the incomplete Bessel function,  $K_0(x, y)$ , which occurs in all the two-electron integrals. Methods then available to us were extremely slow when neither of the arguments  $x$  or  $y$  was less than unity; however, cases with larger  $x$  and  $y$  occur frequently in our calculations, indicating the need for a better algorithm. Recently, one of us (F.E.H.) has developed and computationally implemented a procedure for  $K_0(x, y)$  which is efficient for the full range of its arguments [21, 22]. Direct substitution of the new algorithm into the FTCHAIN program leads consistently to at least a factor 2 in the reduction of the total computing time of test runs on —(Li<sub>2</sub>)<sub>x</sub>— and —(CH<sub>2</sub>—O)<sub>x</sub>— for  $n_k$  values of 17 and 33.

**Table 1.** Exponents and positions (distance from the atom) of the distributed basis set of s-type Gaussian functions (DSGF basis set) for the poly(oxyethylene) translational unit cell.  $s$ -C<sub>2p</sub> and  $s$ -O<sub>2p</sub> are the s-type Gaussian orbitals that simulate the C and O 2p orbitals, respectively. The geometry of the poly(oxyethylene) chain is described in Ref. [16]

Basis function	Exponent	Distance from the atom (Å)
H <sub>1s</sub>	0.27095	0.0
C <sub>1s</sub>	8.71074	0.0
C <sub>2s</sub>	0.25911	0.0
$s$ -C <sub>2p</sub>	0.656	0.55751
O <sub>1s</sub>	15.89814	0.0
O <sub>2s</sub>	0.50786	0.0
$s$ -O <sub>2p</sub>	0.62	0.39822

#### 4.2 Numerical integration in the BZ

In our previous test applications [12–16] it was found that with  $n_k$  equal to 33 ten decimal digits are secured in the one-electron and total energy values. This level of accuracy is certainly higher than actually required in practice. Hence, with the point of view of reducing the computing cost, while still carrying out the lattice summations consistently to convergence, we studied the loss of accuracy accompanying a reduction in  $n_k$ .

From the data in Tables 2 and 3, it appears that  $n_k = 17$  leads to five-decimal-digit accuracy in the energy band values for practically all tests and seven-decimal-digit accuracy for the total energy. In the case of the total energy that level is not attained for the metallic  $-(\text{Li}_2)_x-$  chain, which is not surprising since the band graph exhibits a logarithmic behaviour near the Fermi point. This is obviously difficult to reproduce with an evenly spaced interpolation based on 17  $k$  points only.

For routine applications on classical systems, i.e. fully occupied BZ cases,  $n_k$  equal to 17 is certainly sufficient. As noted in Tables 2 and 3, the computing time ratio,  $r_{\text{CPU}}$ , is reduced by the expected factor 0.27, or  $(17/33)^2$ . It is worth stressing that by simply using the new algorithm for  $K_0(x, y)$  and  $n_k = 17$ , the FTCHAIN program is able to execute on the same computer equipment the test calculations at the same speed as PLH.

At this stage, it is fair to recognise that an efficient and practical way of controlling the accuracy of the numerical integrations in the BZ is still missing. Indeed, carrying out separate calculations with increasing numbers of  $k$  points is no better than the trial-and-error procedures used in direct space to set the lattice summation limits. A promising direction for increasing both the accuracy and cost savings, at least similar to that achieved by reducing  $n_k$  from 33 to 17, is to take advantage of the analytical properties in the BZ of the  $k$ -dependent quantities, especially the two-electron inte-

grals. These quantities are analytic except in metallic (degenerate) cases, where they are only continuous [23–26]. We have noted that the two-electron integrals,  $J_{pqrs}(k, k')$  and  $X_{pqrs}(k, k')$ , vary smoothly in the BZ as suggested by typical graphs shown in Figs. 2 and 3. For  $-(\text{Li}_2)_x-$  with  $s_0 = 10.2$  au, the graphs of  $X_{pqrs}(k, k')$ , are shown in Fig. 2a and those of  $P_{pq}(k)$  are shown in Fig. 2b, where  $p$  and  $s$  correspond to 2s functions

**Table 3.** Valence band energies at selected  $k$  points,  $E_n(k)$  ( $n$  is the band index), and total energy,  $E_T$ , per  $-\text{CH}_2-\text{O}-$  unit for the poly(oxyethylene) chain using 17 and 33  $k$  points in half the first Brillouin zone. All values are in atomic units. *Underlining* is used to highlight differences between the results obtained with  $n_k = 17$  and 33.  $r_{\text{CPU}}$  is the ratio of the total computing time for  $n_k = 17$  to  $n_k = 33$

	$n_k = 17$	$n_k = 33$
$E_3(0.0)$	-1.607974	-1.607978
$E_3(0.125)$	-1.596154	-1.596176
$E_3(0.25)$	-1.564612	-1.564616
$E_3(0.375)$	-1.526498	-1.526519
$E_3(0.5)$	-1.507678	-1.507682
$E_4(0.0)$	-0.886881	-0.886881
$E_4(0.125)$	-0.880786	-0.880803
$E_4(0.25)$	-0.892096	-0.892097
$E_4(0.375)$	-0.959436	-0.959452
$E_4(0.5)$	-0.998490	-0.998492
$E_7(0.0)$	-0.371179	-0.371180
$E_7(0.125)$	-0.375521	-0.375500
$E_7(0.25)$	-0.402694	-0.402695
$E_7(0.375)$	-0.465402	-0.465388
$E_7(0.5)$	-0.524603	-0.524605
$E_8(0.0)$	-0.257598	-0.257600
$E_8(0.125)$	-0.257515	-0.257490
$E_8(0.25)$	-0.266913	-0.266915
$E_8(0.375)$	-0.300679	-0.300667
$E_8(0.5)$	-0.330902	-0.330906
$E_T$	-97.288075	-97.288082
$r_{\text{CPU}}$	0.28	1

**Table 2.** Valence band energies at selected  $k$  points,  $E_n(k)$  ( $n$  is the band index), and total energy per  $-\text{Li}_2-$  unit,  $E_T$ , for the infinite linear chain of lithium molecules,  $-(\text{Li}_2)_x-$ , with  $a_0 = 10.0, 10.2$  and 12.0 au using 17 and 33  $k$  points in half the first Brillouin zone.

	$a_0 = 10.0$ au		$a_0 = 10.2$ au		$a_0 = 12.0$ au	
	$n_k = 17$	$n_k = 33$	$n_k = 17$	$n_k = 33$	$n_k = 17$	$n_k = 33$
$E_3(0.0)$	-0.211777	-0.211777	-0.208131	-0.208136	-0.186767	-0.186767
$E_3(0.125)$	-0.204973	-0.204973	-0.201475	-0.201480	-0.181697	-0.181697
$E_3(0.25)$	-0.183300	-0.183300	-0.180594	-0.180603	-0.166693	-0.166693
$E_3(0.375)$	-0.141711	-0.141711	-0.143195	-0.143189	-0.144405	-0.144405
$E_3(0.5)$	-0.056198	-0.056198	-0.105636	-0.105568	-0.130254	-0.130255
$E_4(0.0)$	0.273511	0.273511	0.262249	0.262251	0.183027	0.183027
$E_4(0.125)$	0.225370	0.225370	0.217220	0.217222	0.159045	0.159045
$E_4(0.25)$	0.132974	0.132974	0.129349	0.129355	0.105930	0.105930
$E_4(0.375)$	0.044510	0.044510	0.046635	0.046627	0.053447	0.053447
$E_4(0.5)$	-0.056198	-0.056198	-0.005751	-0.005821	0.028532	0.028533
$E_T$	-14.617868	-14.617922	-14.621426	-14.621426	-14.624779	-14.624778
$r_{\text{CPU}}$	0.27	1	0.27	1	0.28	1

All values are in atomic units. *Underlining* is used to highlight differences between the results obtained with  $n_k = 17$  and 33.  $r_{\text{CPU}}$  is the ratio of the total computing time for  $n_k = 17$  to  $n_k = 33$

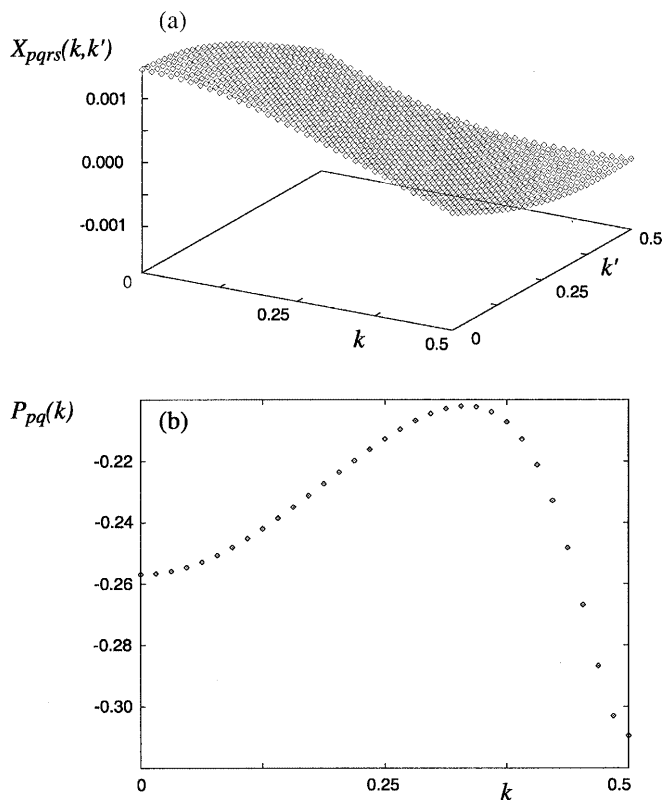


**Fig. 2.** Graphs of **a**  $X_{pqrs}(k, k')$  and **b**  $P_{pq}(k)$  functions in half the BZ for the  $-(\text{Li}_2)_x-$  chain ( $s_0 = 10.2$  au)

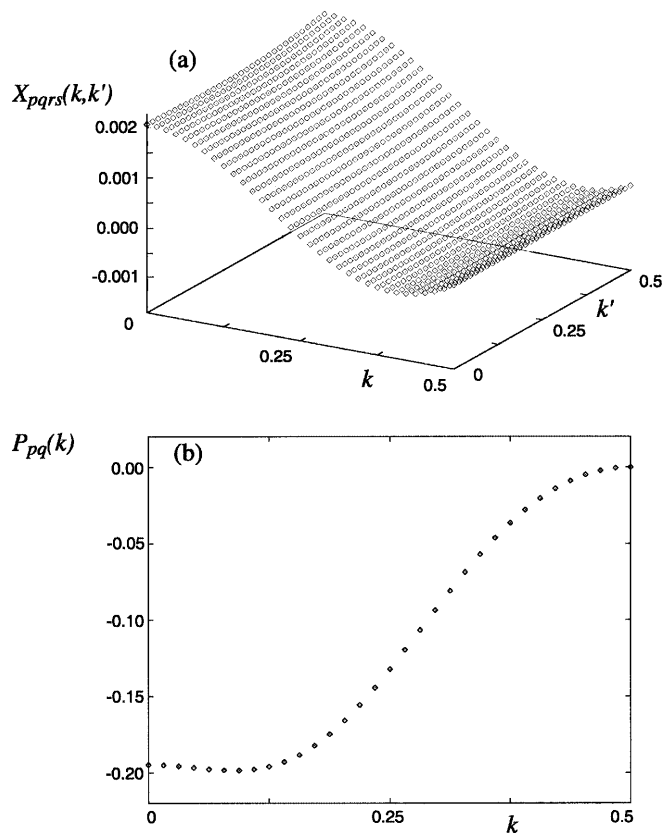


**Fig. 3.** Graphs of **a**  $X_{pqrs}(k, k')$  and **b**  $P_{pq}(k)$  functions in half the BZ for the  $-(\text{CH}_2\text{-O})_x-$  chain

centred on one of the lithium atoms and  $q$  and  $r$  to 1s functions located on the other atom. Similar quantities for the  $-(\text{CH}_2\text{-O})_x-$  chain are represented in Figs. 3a and b, where  $p$ ,  $q$  and  $r$  are 2p atomic functions centred on the carbon atom, while  $s$  corresponds to the 1s function located on one of the two equivalent hydrogen atoms. For each of these two illustrative cases, the selected  $pqrs$  quadruples correspond to the  $X_{pqrs}(k, k')$  integrals of largest variation in the BZ out of the full list of  $J_{pqrs}(k, k')$  and  $X_{pqrs}(k, k')$  integrals. The  $P_{pq}(k)$  density matrix elements correspond to the first two atomic indices of these selected integrals. It is important to note that the integrals (Figs. 2a, 3a) are quite smooth in contrast to the  $P_{pq}(k)$  functions. Furthermore, as already stressed, the  $J_{pqrs}(k, k')$  and  $X_{pqrs}(k, k')$  integrals are those actually responsible for the bulk of the total computational effort. Hence it is conceivable to start from a grid containing a somewhat reduced number of  $(k, k')$  points, for example,  $n_k^2$  with  $n_k = 17$ , and to fill by two dimensional interpolation the missing values in a table that would contain  $n_k^2$  points, for example  $n_k' = 33$ . These values would be integrated after multiplication with the more widely varying  $k$ -dependent density matrices,  $P_{rs}(k')$  (see Eqs. 15, 16). These observations, which correspond to similar suggestions made by te Velde, open the prospect of constructing an adaptive numerical integration technique from which the accuracy of numerical integrations in the BZ would be controlled within a single calculation instead of repeating separate calculations.

## 5 Concluding remarks

In this article we have provided the general expressions for s-type Gaussian bases needed to carry out Fourier-space RHF-LCAO band structure calculations on general systems of one-dimensional periodicity. After introducing a new algorithm for the calculation of the incomplete Bessel function,  $K_0(x, y)$ , and using a more realistic number of integration points in the BZ, the Fourier-space RHF-LCAO code (FTCHAIN) efficiency appears to be comparable to that of the existing direct-space versions, such as PLH and CRYSTAL95. In such comparisons, the standard settings of the PLH program were used. In both FTCHAIN and PLH, prescreening based on the magnitude of the overlap matrix elements is used. An important advantage of FTCHAIN, however, is that all lattice summations are computed consistently and to a desired accuracy, thus avoiding the use of approximate expressions (multipolar expansions, etc.) and setting summations limits by trial and error.

Interpolation in the  $(k, k')$  plane of the two-electron integrals  $J_{pqrs}(k, k')$  and  $X_{pqrs}(k, k')$ , which is possible due to smooth variation of these terms, and a more careful definition of the various thresholds for the various LCAO integrals, opens the prospect of further efficiency increases. This, however, will be postponed until after implementation of expressions for atomic functions of higher quantum number (p, d, ...) [12].

*Acknowledgements.* The calculations reported were carried out at the Namur Scientific Computing Facility with the financial support of the FNRS-FRFC, the Loterie Nationale (9.4553.92) and the FNRS/Belgian Ministry of Science Action d'impulsion à la recherche fondamentale (D.4511.93). We thank G. te Velde of Vrije Universiteit, Amsterdam, for an insightful discussion, and F.E.H. gratefully acknowledges the hospitality extended to him at FUNDP, Namur.

## References

1. André JM, Delhalle J, Brédas JL (1991) Quantum chemistry aided design of organic polymers. World Scientific, London
2. Piela L, Delhalle J (1978) *Int J Quantum Chem* 13: 605
3. Delhalle J, Fripiat JG, Piela L (1980) *Int J Quantum Chem* 14: 431
4. Pisani C, Dovesi R, Roetti C (1988) In: Hartree-Fock ab initio treatment of crystalline systems, Lecture Notes in Chemistry, vol. 48. Springer, Berlin Heidelberg New York
5. Teramae H (1996) *Theor Chim Acta* 94: 311
6. Sun JQ, Bartlett RJ (1996) *J Chem Phys* 104: 8553
7. Harris FE, Monkhorst HJ (1970) *Phys Rev B* 2: 4400
8. Harris FE (1972) *J Chem Phys* 56: 4422
9. Delhalle J, Harris FE (1978) *Theor Chim Acta* 48: 127
10. Delhalle J, Harris FE (1985) *Phys Rev B* 31: 6755
11. Delhalle J, Cizek J, Flamant I, Calais JL, Fripiat JG (1994) *J Chem Phys* 101: 10717
12. Flamant I (1998) PhD thesis. Presses Universitaires de Namur, University of Namur
13. Flamant I, Fripiat JG, Delhalle J (1996) *Int J Quantum Chem* 60: 1487
14. Flamant I, Delhalle J, Fripiat JG (1997) *Int J Quantum Chem* 63: 709
15. Flamant I, Fripiat JG, Delhalle J (1997) *Theor Chem Acc* 98: 155
16. Flamant I, Fripiat JG, Delhalle J (1998) *Int J Quantum Chem* 70: 1045
17. Fripiat JG, Mosley DH, Champagne B, André JM PLH-93 from METECC-94
18. Dovesi R, Saunders VR, Roetti C, Causà M, Harrison NM, Orlando R, Aprà E (1996) Crystal95 user's manual. University of Torino, Torino
19. Agrest MM, Maksimov MS (1971) Theory of incomplete cylindrical functions and their applications. Springer, Berlin Heidelberg New York
20. Abramowitz M, Stegun I (1964) Handbook of mathematical functions. Dover, New York
21. Harris FE (1997) *Int J Quantum Chem* 63: 913
22. Harris FE (1998) *Int J Quantum Chem* 70: 623
23. Kohn W (1959) *Phys Rev* 115: 1460
24. Bulyanitsa DS, Svetlow Yu E (1962) *Sov Phys Solid State* 4: 981
25. Des Cloizeaux J (1963) *Phys Rev* 129: 554
26. (a) Des Cloizeaux J (1964) *Phys Rev A* 135: 685; (b) Des Cloizeaux J (1964) *Phys Rev A* 135: 698